27 May 2010, 4:30 pm - 6:20 pm

The Effect of Geometry Changes on Sliding-Block Predictions

Constantine A. Stamatopoulos
Hellenic Open University, Greece

Constantine Mavromihalis
Hellenic Open University, Greece

Sarada Sarma
Imperial College, London, U.K.

Fifth International Conference on
Recent Advances in Geotechnical Earthquake Engineering and Soil Dynamics
and Symposium in Honor of Professor I.M. Idriss
May 24-29, 2010 • San Diego, California

THE EFFECT OF GEOMETRY CHANGES ON SLIDING-BLOCK PREDICTIONS

Constantine A. Stamatopoulos
Instructor, Hellenic Open University
5 Isavron st, 114 71 Athens, GREECE

Constantine Mavromihalis
Student, Hellenic Open University
29 28th October st , Thessaloniki, 57500, Greece

Sarada Sarma
Imperial College
London, UK

ABSTRACT

The sliding-block model is often used for the prediction of permanent co-seismic displacements of slopes and earth structures. This model assumes motion in an inclined plane but does not consider the decrease in inclination of the sliding soil mass as a result of its downward motion, which is the usual state in the field. The paper studies the above effect and proposes an empirical equation correcting the predictions of the sliding-block model. The investigation is performed using the recently-developed multi-block model.

INTRODUCTION

Permanent seismic movement of slopes can be separated into at least two stages (Ambraseys and Srbulov, 1995). In the first stage, which is co-seismic, gravity in combination with transient seismic forces may bring about temporary instability and permanent displacements on a failure surface. The second stage, which is post-seismic, follows immediately after the earthquake and causes large movement if, as a result of the first stage, the strength on the slip surface is reduced to a residual value which is less than that required to maintain static equilibrium.

The sliding-block method, that was initially proposed by Newmark (1965) forms the basis of simple models predicting permanent co-seismic displacements of slopes. As shown in Fig. 1, a block with resistance simulated by the Mohr-Coulomb law rests on an inclined plane. Critical acceleration is defined as the minimum horizontal acceleration that causes movement of the block. During each time that the applied horizontal acceleration is larger than the critical acceleration, the block slides. The total displacement of the block is obtained by the addition of the partial slips. This model has been used for the estimation of permanent seismic deformations of natural slopes without considerable earthquake-induced loss of strength (Ambraseys and Srbulov, 1995), of earth dams (Sarma ,1975, Makdisi and Seed, 1978), of rockfill dams (Gazetas and Dakoulas, 1992) and of gravity walls retaining dry soil (Richards and Elms, 1979). The solutions giving the distance moved by the sliding-block are used for the prediction of permanent seismic movement of these problems by replacing the maximum applied acceleration and critical acceleration of the block with those of the potential sliding mass under consideration. The critical acceleration of the sliding mass is estimated by stability or limit-plasticity analyses and the maximum applied acceleration is often obtained by dynamic analyses.

The sliding-block model is generally successful in estimating small ground deformations without earthquake-induced loss of strength (Whitman, 1993). However, when the ground displacement is large, it is not accurate, primarily because of (a) earthquake-induced loss of strength in saturated soils and (b) changes of geometry of the soil mass towards a gentler inclination. Various efforts have been made to incorporate the first effect in the estimation of co-seismic displacements taking into account loss of shear strength (Makdisi and Seed, 1978, Tika-Vassilikos et al., 1993) and/or pore-pressure build-up (Sarma, 1975, Modaressi et al., 1995).

The second effect is the usual state in slides in the field, and is caused by the law of physical equilibrium where masses move towards a more stable configuration. It reduces seismic displacement and is considerable when displacements are large. It has been studied by Stamatopoulos (1996). The study considered a perfectly flexible chain sliding along planes with gradually gentler inclinations. The cases of ground slips where the permanent displacement of the new model differs considerably from that of the sliding-block model were detected and an improved method predicting permanent seismic displacement was proposed. Yet, in this work the governing equation of motion of the new model was approximately derived and solved and rigorous factors correcting the predictions of the sliding-block model were not obtained.

To simulate slope movement when displacement is large, two-block (Stamatopoulos, 1992, Ambraseys and Srbulov, 1995,

Stamatopoulos et al., 2000) and multi-block (Sarma and Chlimintzas, 2001) sliding models have been proposed and solved. The multi-block model is the most general. It is described below.

The paper studies the effect of the change of geometry during the slide on the seismic displacement predicted by the sliding-block model and proposes factors that correct the seismic displacement predicted by the sliding-block model. The investigation is performed using the recently-developed multi-block model. The methodogy used is the following: (a) obtain a factor describing the effect of the change in geometry of the slope with displacement by formulating the equation of motion of the multi-block model for a simplified geometry, (b) by applying the multi-block model in a parametric manner, investigate quantitavely the effect that the above factor has in the ratio $u_f/u_{f\text{-}o}$, where u_f and $u_{f\text{-}o}$ is the final displacement predicted when geometry changes are and are not considered respectively and (c) formulate an empirical equation describing the effect computed in (b).

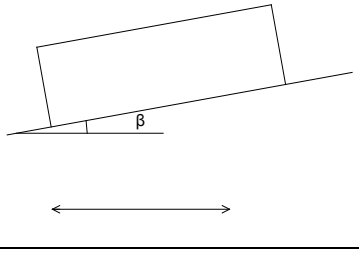

Fig. 1. Newmark's sliding-block model

THE MULTI-BLOCK SLIDING SYSTEM AND THE ASSOCIATED COMPUTER PROGRAM

Similarly to the Sarma (1979) stability method, shown in Fig. 2, a general mass sliding on a slip surface that consists of n linear segments is considered. In order the mass to move, at the nodes between the linear segments, interfaces where resisting forces are exerted must be formed. Thus, the mass is divided into n blocks sliding in different inclinations. When the slide moves, at the interface between two consecutive blocks, the velocity must be continuous. This principle gives that the relative displacement of the n blocks is related to each other as:

$$u_i/u_{i+1} = du_i/du_{i+1} = \cos(\beta_{i+1}+\delta_i) / \cos(\beta_i +\delta_i) \qquad (1)$$

where the subscripts i and i+1 refer to blocks i and i+1 counting uphill, d refers to increment, β_i is the acute angle of the slip surface segment at slice i, positive anti-clockwise when measured from the horizontal to the slip surface and δ_i is the acute angle between the vertical and the interslice surface of blocks i and i+1, measured from the vertical, positive clockwise, shown in Fig. 2.

The forces that are exerted in block "i" are given in Fig. 2. Soil is assumed to behave as a Mohr-Coulomb material. As the body moves, the Mohr Coulomb failure criterion applies at both the slip surface and the interfaces. Thus, the equation of motion of each body can be derived. To eliminate the interslice forces, N_i, the equations are multiplied by a factor. Summing all equations and expressing displacement of all blocks in terms of the displacement of the upper block, the equation of motion is obtained. In the present study (a) a horizontal acceleration (k(t)g is applied, where g is the acceleration of gravity and k(t) is the horizontal seismic coefficient in terms of time, (b) motion is assumed to take place only in the downward direction and (c) separation of blocks does not occur. In this case, as given by Sarma and Chlimitzas (2001), the governing equation of motion is

$$\ddot{u}(t)\cdot\sum_{i=1}^{n}\left(m_i q_i\cos(\varphi_i')\cdot\prod_{j=i}^{n-1}\frac{\bar{d}_{j+1}}{\bar{f}_j}\right)=\sum_{i=1}^{n-1}\left(\left[-\bar{c}_i' b_i\cos(\bar{\varphi}_i')+\bar{U}_i\sin(\bar{\varphi}_i')\right]\cdot\frac{\bar{s}_i}{\bar{f}_i}\cdot\prod_{j=i+1}^{n-1}\frac{\bar{d}_{j+1}}{\bar{f}_j}\right)+$$
$$+\sum_{i=1}^{n}\left(\left\{\bar{x}_i(m_i g k(t)+H_i)-\bar{v}_i[m_i g+Q_i]-c_i' l_i\cos(\varphi_i')+U_i\sin(\varphi_i')\right\}\cdot\prod_{j=i}^{n-1}\frac{\bar{d}_{j+1}}{\bar{f}_j}\right) \qquad (2)$$

where

$$\bar{s}_i=\sin(\beta_{i+1}-\beta_i+\phi_i'-\phi_{i+1}')$$
$$\bar{f}_i=\cos(\phi_i'+\bar{\varphi}_i'-\beta_i-\delta_i)$$
$$\bar{d}_i=\cos(\phi_i'+\bar{\varphi}_{i-1}'-\beta_i-\delta_{i-1})$$
$$\bar{x}_i=\cos(\phi_i'-\beta_i)$$
$$\bar{v}_i=\sin(\phi_i'-\beta_i)$$
$$q_i=\prod_{j=i}^{n-1}\frac{\cos(\beta_{j+1}+\delta_j)}{\cos(\beta_j+\delta_j)}$$

where u is the relative shear displacement of the uppermost slice (block n), down-hill displacements being considered positive, β_i and δ_i were defined previously φ_i' is the angle of friction on the slip surface at slice i, $c_i'l_i$ is the force per unit length (normal to the paper) due to cohesion along the slip surface at block i, $\bar{\varphi}_i'$ is the angle of friction on the interslice surface between blocks i and i+1, $\bar{c}_i' b_i$ is the force per unit length due to cohesion along the interslice surface between blocks i and i+1, Q_i is the vertical external load on slice i, positive downwards, H_i is horizontal external load on slice i, positive facing downhill, m_i is the mass of block (slice) i per unit length, U_i is the force acting on slice i, normal to its base due to pore water pressures along the slip surface, positive when normal component is compressive and $\bar{U}_i$ is the pore water force along the interface between slices i and i+1 that acts in a direction normal to it, positive when normal component is compressive.

It should be noted that equation (2) can be written in the form

$$\ddot{u}_1 = Z_1\, g\,(k(t) - k_c) \qquad (3)$$

where

$$Z_1 = \frac{\{-\bar{x}_i(m_i g)\}\cdot\prod_{j=i}^{n-1}\frac{\bar{d}_{j+1}}{\bar{f}_j}}{\sum_{i=1}^{n}\left(m_i q_i\cos(\varphi_i')\cdot\prod_{j=i}^{n-1}\frac{\bar{d}_{j+1}}{\bar{f}_j}\right)}$$

$$\sum_{i=1}^{n-1}\left(\left[\bar{c}_i' b_i\cos(\bar{\varphi}_i')-\bar{U}_i\sin(\bar{\varphi}_i')\right]\cdot\frac{\bar{s}_i}{\bar{f}_i}\cdot\prod_{j=i+1}^{n-1}\frac{\bar{d}_{j+1}}{\bar{f}_j}\right)+$$

$$k_c = \frac{\sum_{i=1}^{n}\left(\{-\bar{x}_i(H_i)+\bar{v}_i[W+Q_i]+c_i' l_i\cos(\varphi_i')-U_i\sin(\varphi_i')\}\cdot\prod_{j=i}^{n-1}\frac{\bar{d}_{j+1}}{\bar{f}_j}\right)}{\{-\bar{x}_i(m_i g)\}\cdot\prod_{j=i}^{n-1}\frac{\bar{d}_{j+1}}{\bar{f}_j}}$$

where k_c is the critical acceleration factor, defined as the horizontal acceleration coefficient needed to initiate motion.

To solve equation (3) for large displacement, the masses and lengths of each block i must be updated in terms of the distance moved. The transformation rule, that states that when each block is displaced by d_i, each point of the block including the ground surface (corresponds to the top of the block) is also displaced by d_i, is applied. In the general case, incremental application of the rule is needed because a point may move from one block to the previous, and thus its incremental displacement for given du_n will change from du_i to du_{i-1}. When mass is transferred from block i to block i-1 equation (1) applies.

In mathematical terms, to solve equation (2) for large displacement it is needed to express the l_i, b_i and m_i in terms of the distance moved, u. Assuming that u is less than the initial length of l_n, the change of lengths l_i in each increment Δu equals

$$\Delta l_1 = \Delta u\, q_1 \quad , \quad \Delta l_n = -\Delta u \qquad (4)$$
$$\Delta l_2 = \Delta l_3 = \ldots\ldots = \Delta l_{n-1} = 0.$$

Furthermore, the change in the internal lengths b_i is

$$\Delta b_i = \frac{\sin\theta_i}{\cos(\theta_i+\beta_i+\delta_i)}\cdot q_i\Delta u_i \qquad (5)$$

and the change in cross-sectional areas of the blocks is :

$$\Delta A_i = b_{(i+1)0}\cdot\cos(\beta_{i+1}+\delta_{i+1})\cdot q_i\Delta u_i + \frac{0.5\cdot\cos(\beta_{i+1}+\delta_{i+1})\cdot\sin\theta_{i+1}}{\cos(\theta_{i+1}+\beta_{i+1}+\delta_{i+1})}\cdot(q_i\Delta u_i)^2 - b_{i0}\cdot\cos(\beta_i+\delta_i)\cdot q_i\Delta u_i - \frac{0.5\cdot\cos(\beta_i+\delta_i)\cdot\sin\theta_i}{\cos(\theta_i+\beta_i+\delta_i)}\cdot(q_i\Delta u_i)^2 \qquad (6)$$

The change of masses can be estimated from ΔA_i as:

$$\Delta m_i = \Delta A_i * \rho_{i+1} \qquad (7)$$

where ρ_{i+1} is the total unit weight of the soil of block i+1. The deformation that this rule predicts in a two-block system is illustrated in Fig. 3.

For very small displacement, equation (3) can be approximated as

$$\ddot{u}_1 = Z_{1\text{-}o}\, g\,(k(t) - k_{c\text{-}o}) \qquad (8)$$

where $Z_{1\text{-}o}$ and $k_{c\text{-}o}$ are the factors Z_1 and k_c given by equation (3) when l_i, b_i and m_i are equal to their initial values, $l_{i\text{-}o}$, $b_{i\text{-}o}$ and $m_{i\text{-}o}$ respectively.

At the point is should be noted that the general equation of motion of Newmark's sliding-block model (Stamatopoulos, 2003) is given by equation (8) with

$$Z1\text{-}o = \frac{\cos(\phi-\beta)\cos\beta}{\cos\phi}$$
$$kc\text{-}o = \frac{m*g*\sin(\phi-\beta)+cl\cos\phi}{mg\cos(\phi-\beta)} \qquad (9)$$

where β is the inclination of the block, φ' and c' is the friction and cohesion along the slip surface and l is the length of the block. It is observed that the multi-block model for small displacement has the form of the conventional sliding-block model. Thus, for small displacement, and given strength and geometry characteristics, an inclination, friction angle and cohesion can be found for the sliding-block model for equivalent response to the multi-block model.

A computer program that solves equations (3) to (7) has been developed by Stamatopoulos. Equation (3) is a second order differential equation. It is solved numerically by the Euler method (e.g. Dahliquis and Bjorck, 1974). The program has the option to consider and not to consider geometry changes. The input geometry is specified as the nodes of the linear segments defining the slip, ground and water table surfaces. The inclinations of the internal slip surfaces are also specified. The unit density and the cohesional and frictional components of resistance are specified for each block. The computer program includes graphics that illustrate (a) the initial and final deformed configurations of the slope and (b) the applied acceleration, the critical acceleration and the mass, acceleration, velocity and displacement of each block, all versus time.

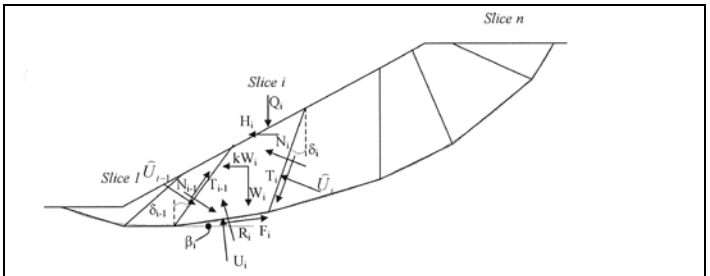

Fig. 2. The multi-block stability method proposed by Sarma (1979).

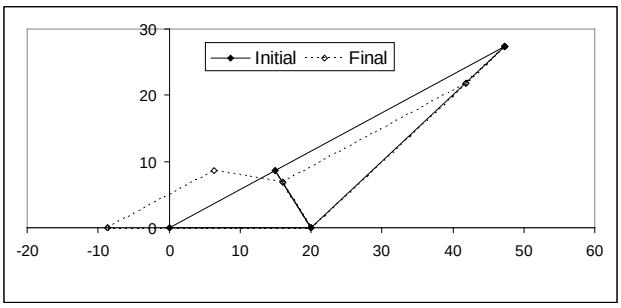

Fig. 3. Deformation assumed in the multi-block model. A case of two blocks is given.

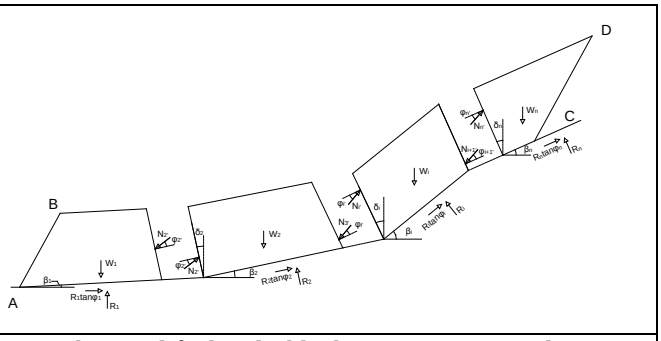

Fig. 4. The simplified multi-block geometry assumed to derive the analytical solution.

FACTOR GOVERNING THE SOLUTION OF A SIMPLIFIED CASE

Simplified case

The governing equation of motion greatly simplifies if (a) $\varphi'_i = 0$, (b) $\delta_i = -(\beta_i + \beta_{i-1})/2$, (c) $\theta_1=\theta_2=...=0$, (d) the side of the slope of the first body (line AB of Fig. 4) is parallel to the side of the last body (line CD of Fig. 4), (e) the density of the sliding mass is uniform (f) pore water pressures are not present and (g) external forces do not exist. Fig. 4 illustrates the geometry of this simplified case.

Provision (a) indicates that resistance is only cohesional. Provision (b) means that the interface angle bisects the angles formed by the slip surface and the distance moved by all bodies is the same ($u_1=u_2=...u_n=u$). Provision (c) indicates that the ground surface is parallel to the slip surface and ensures a linear change of the geometric lengths with the distance moved.

As a result of provisions (a) and (b):

$$q_i=1, \quad \cos(\varphi'_i)=1, \quad \prod_{j=i}^{n-1} \frac{\bar{d}_{j+1}}{\bar{f}_j}=1, \qquad (10)$$

$$\bar{v}_i = -\sin(\beta_i), \quad \bar{x}_i = \cos(\beta_i),$$

$$\bar{s}_i = \sin(\beta_{i+1} - \beta_i), \; \bar{f}_i = \cos(-\beta_i - \delta_i)$$

As a result of provisions (c), (d) and (e)

$l_1=l_{1-o} + u$
$l_n=l_{n-o} - u$

where l_{1-o} and l_{n-o} are the initial values of l_1 and l_n. In addition, the lenghts l_2, l_3, .., l_{n-1}, as well as the internal lengths b_i do not change. In addition, the masses of the blocks equal:

$$m_1= m_{1-o} + u \rho b_{2o} \cos(\beta 2+\delta 2) = m_{1o} + u\, m_{tot} / l \qquad (12)$$
$$m_n= m_{n-o} - u\, m_{tot} / l$$

where l is the slip length and m_{1-o} and m_{n-o} are the initial values of m_1 and m_n. In addition, the areas m_2, m_3,.....m_{n-1} do not change.

As a result of provision (f)

$$U_i = \hat{U}_i = 0 \qquad (13)$$

Furthermore, provision (g) gives that

$$H_i=P_i=0 \qquad (14)$$

Thus, the equation of motion becomes

$$\ddot{u}(t)\cdot m_{total} = \sum_{i=1}^{n-1}\left(\left[\bar{c}'_i b_i\right]\cdot \frac{\bar{s}_i}{\bar{f}_i}\cdot \right) + \sum_{i=1}^{n}\left(\left\{ \left(m_i g(-k(t)\cos\beta_i + \sin\beta_i)\right) + c'_i l_i \right\}\right) \qquad (15)$$

Where m_{tot} is the total mass of the slide. Replacing the mass and lengths with its initial value and their change with the distance moved, the governing equation of motion becomes

$$\ddot{u}(t) = \sum_{i=1}^{n-1}\left(\left[\bar{c}'_i b_{i-o}\right]\cdot \frac{\bar{s}_i}{\bar{f}_i}\cdot \right) / m_{total} + \sum_{i=1}^{n}\left(\left\{ \left(m_{i-o} g(-k(t)\cos\beta_i + \sin\beta_i)\right) + c'_i l_{i-o} \right\}\right) / m_{total} + u\cdot g\{-k(t)(\cos\beta_1 - \cos\beta_n) + \sin\beta_1 - \sin\beta_n\} / l \qquad (16)$$

where m_{i-o} is the initial value of the mass m_i.

At this point it should be noted that if mass change is not considered, equation (16) is reduced to

$$\ddot{u}(t) = \sum_{i=1}^{n-1}\left(\left[\bar{c}'_i b_{i-o}\right]\cdot \frac{\bar{s}_i}{\bar{f}_i}\cdot \right) / m_{total} + \sum_{i=1}^{n}\left(\left\{ \left(m_{i-o} g(-k(t)\cos\beta_i + \sin\beta_i)\right) + c'_i l_{i-o} \right\}\right) / m_{total} \qquad (17)$$

Discussion

It was noted previously that the equation of motion of the multi-block model for small displacement has the form of the conventional sliding-block model. Furthermore, for the case of large displacement and the simplified geometry of Fig. 4, equations (16) and (17) illustrate that the equation of motion changes (as a result of geometry changes during motion) by the factor

F1= $u \cdot g\{-k(t)(\cos\beta_1 - \cos\beta_n) + \sin\beta_1 - \sin\beta_n\} / l$ (18)

The effect of the change of geometry of the slope during motion on the seismic displacement will be described by the rario u_f/u_{f-o}, where u_f is the final displacement moved by the multi-block model as a result of the applied exhitation k(t), while u_{f-o} is the corresponding displacement when geometric changes are not considered. Equation (8) indicates that uo depends on the factors k(t), k_{c-o} and Z_{1-o}. Furthermore, equations (16) and (17) indicate that u_f for the simplified geometry depends, in addition to the factors k(t), k_{c-o} and $Z_{1-o,}$ on the factors F1.

Fig 5 studies the correlation between the factors $(\sin\beta_n - \sin\beta_1)$ and $(\cos\beta_n - \cos\beta_1)$ with the factor $(\beta_n - \beta_1)$. The angle β_1 is taken to vary between 0 and 40^o and the angle βn between 0 and 45^o at 5 degree increments (under the condition $\beta_n > \beta_1$). It is observed that there is strong correlation between the factors (i) $(\sin\beta_n - \sin\beta_1)$ and ((ii) $\cos\beta_n - \cos\beta_1$) with the factor $(\beta_n - \beta_1)$. Furthermore, it is observed that $(\sin\beta_n - \sin\beta_1) > 2$ (cosβn - cosβ1). In addition, the factor k usually varies between the values +/-0.5. It is inferred that the first factor affects the factor F1 much more than the second factor. Based on the above, it is inferred that the factor F1 is approximately proportional to the factor

F2= u $(\beta_n - \beta_1) / l$ (19)

The displacement u of the factor F2 increases with time and finally gets the value u_f. It is inferred that an average value of u is the $u_f/2$. Furthermore, the displacement u_f can be approximated by $u_{f-o,}$ that can be obtained from the previously commonly-used sliding-block model. Thus, the factor F2 is approximately proportional to

F= u_{f-o} (βn - β1) / l (20)

The factor F will be used below to describe the effect of the geometry and strength of the slope, as well as of the applied exhitation on the ratio u_f/u_{f-o}, defined above. The geometry affects F by the length of the slip surface and the difference in inclination of the last (upper) and first (lower) linear segments of the slip surface. The applied exhitation affects F indirectly, by the seismic displacement, u_{f-o}. It is observed that the factor F tends to zero when (1) the seismic displacement is very small, (2) the length of the slip surface is very large and (3) the difference in inclination of the last (upper) and first (lower) blocks of the slip sub-planes of the slope is very small. Indeed, in all these three cases the effect of the change of geometry of the slide during motion at the seismic displacement diminishes, and thus. u_f/u_{f-o} equals to one.

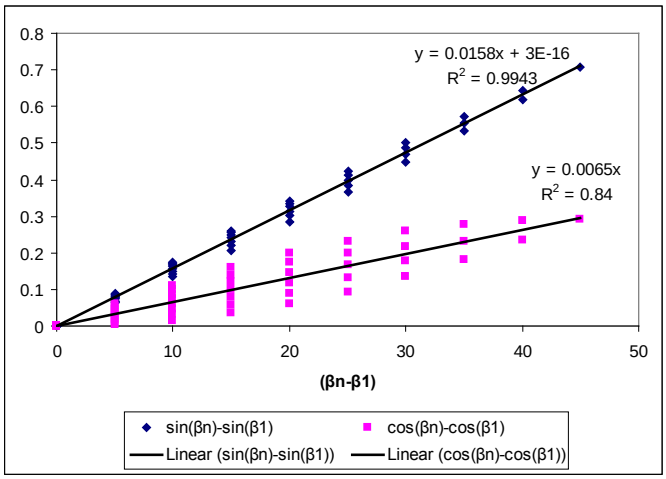

Fig. 5 The correlation between the factors $(\sin\beta n - \sin\beta 1)$ and $(\cos\beta n - \cos\beta 1)$ with the factor $(\beta n - \beta 1)$.

PARAMETRIC ANALYSES

The manner that the factor F derived above affects the actual results of the ratio u_f/u_{f-o} defined above is investigated by applying the computer program assosiated with the multi-block model (section 2). The two-block geometry of Fig. 6 is considered. From Fig.6, it is observed that this geometry is defined by the parameters β_1, β_2 ($=\beta_n$), δ, θ, l ($=l_1+l_2$) and wte (water table elevation). All these parameters were varied in a parametric manner. The initial and main case considered in the parametric analyses had the following characteristics: δ=-10^o, β_1=5^o, β_2=40^o, θ=30^o, l=20m, wte=0. For each other case considered in the parametric analysis only one parameter was varied. In all cases the El-Centro accelerogram was applied. Table 1 gives the cases that were considered in the parametric analysis of the geometry of fig. 6

The methodology of solution for each case solved when varying β_1, β_2, δ, θ, l, was the following: The friction is taken zero and the cohesion is taken the same along both the two sub-planes of the slip surface and the interface. We prepare an input file that describes the geometry considered and we estimate by trial-and-error the limit minimum value of cohesion (c') that gives positive critical acceleration, and lies necessarily between 0 and 0.01g. Then, we increase the value of cohesion c' with small increments multiplying by 1.05 each time. When the critical acceleration exceeds the maximum acceleration of the applied accelerogram, the analysis stops, as the seismic displacement is zero. For each case of c the final displacement (u_f),, the corresponding displacement if mass transfer is not considered (u_{f-o}) and the factor F are recorded.

As changes in wte do not affect the cohesional resistance force, the methodology of solution when varying the wte was the following: The cohesion is taken zero and the friction is taken the same along both the two sub-planes of the slip surface and the interface. We prepare an input file that describes the geometry considered and we estimate by trial-and-error the limit minimum value of φ' that gives positive critical acceleration, and lies necessarily between 0 and 0.01g.

Then, we increase the value of φ' with small increments multiplying by 1.1 each time. When the critical acceleration exceeds the maximum acceleration of the applied accelerogram, the analysis stops, as the seismic displacement is zero. For each case of φ', the final displacements u_f and u_{f-o} and the factor F are recorded.

The effect of varying the cohesion (and also the friction angle) was also studied. The procedure used was the following: The friction and the cohesion is taken the same along both the two sub-planes of the slip surface and the interface. First we prepare an input file that describes the geometry considered and for c a given value we estimate by trial-and-error the limit minimum value of φ' that gives positive critical acceleration, and lies necessarily between 0 and 0.01g. Then, we increase the value of friction with small increments multiplying by 1.1 each time. When the critical acceleration exceeds the maximum acceleration of the applied accelerogram, the analysis stops, as the seismic displacement is zero. For each case of φ' the final displacement (u_f), as well as the corresponding displacement if mass transfer is not considered (u_{f-o}) are recorded

As stated above, for each case considered in the parametric analysis only one parameter was varied from the initial run. This means that, for example for the case of analysis in terms of the parameter δ, the other parameters remain unchanged, i.e. $\beta_1=5^o$, $\beta_2=40^o$, $\theta=30^o$, l=20m, wte=0 and only the angle δ varies. In this manner, the results of the parametric analyses for $\delta=-40^o$, -30^o, -20^o, -10^o, 0^o, 10^o, 20^o, 30^o are derived. The results of the analyses, i.e. the relationship between the ratio (u_f/u_{f-o}) and the factor F in terms of the parameter that was varied, are given in Figs. 7 and 8 for all cases considered.

PROPOSED EMPIRICAL EXPRESSION

Proposed form of the expression

In all results of Figs. 7 and 8, it is observed that (a) if the factor F is smaller than a particular value, Fo, the ratio (u_f/u_{f-o}) equals to unity and (b) when F is larger than Fo, as F increases further, the ratio (u_f/u_{f-o}) gradually decreases from unity towards zero, forming an S-shape curve in the logarithmic (in terms of F) scale.

The shape of this relation is similar to the well-known relation of soil dynamics between G/Gmax and γ, where G is the shear modulus at the curent shear strain level, Gmax is the elastic shear modulus at very small shear strain and γ is the shear strain. The G/Gmax versus γ curve has been modeled with analytical equations of the form

$$G/Gmax= 0.5 \tanh [1+ (\ln (A'/\gamma)B'] \quad (21)$$

where A', B' are parameters (Ishibishi and Zhang , 1993). Similarly, the results of the present study will be described with the relationship

$$(u_f/u_{f-o}) = 0.5 \tanh [1+ (\ln (A/F)B] \quad (22)$$

where F is the factor given by equation (20) and A, B are best-fit parameters.

From Figs. 7 and 8 it can be observed that the relationship between ratio (u_f/u_{f-o}) and the factor F does not vary considerably as the parameters of the geometry of Fig. 6 vary, except from the parameter l. In all other cases the curves of (u_f/u_{f-o}) versus the factor F are almost identical. It is inferred that the parameters A and B may vary only with the slip length l.

Best-Fit values of the parameters A and B

Fig. 9a gives the results of all analyses except from those with the slip length l. In particular, the parameters β1, β2, θ, δ, wte, φ' and c' vary, while l=20m. Trial and error gave that the parameters that best fit the results are

$$A=1.5 \text{ and } B=0.56 \quad (23)$$

Fig. 9a gives the prediction of equation (22) with A=1.5 and B=0.56. It can be observed that the proposed equation with the proposed parameters fits well all results of the numerical analysis of all parametric analyses, except of those of varying l.

In addition, the predicted values (P) are given in terms of the real (X) values computed by the numerical analyses assuming linear relation

$$P = C X \quad (24)$$

where C is a parameter. The parameter C, but also the coefficient of correlation (R^2) must be close to unity for satisfactory prediction. Fig. 9b gives that C=0.9957 and R2=0.9969. The two parameters are very close to unity and this indicates that the correlation is very good. In addition, table 1 gives gives the values of C and R^2 for all curves of Figs 7 and 8 separately. It can be observed, consistently to the above, that C and R^2 are very close to unity for all cases, except from some cases where the factor l was varied.

Up to now, the proposed values of the fitting parameters A and B of equation (22) do not consider the effect of the slip length, l, that is considerable. This effect is studied separately. It is observed that to fit the results, it is sufficient to vary only the parameter A in terms of l. First, for each l the value of the parameter A that predicts the results better was found. It is given in table 2. The predicted values are compared with the computed values for each value of l using the optimum value of A again with equation (24). Table 2 gives the number of cases (N) and correlation (the factor C and the coefficient of correlation R^2) for the optimum A for each l value. It can be observed that C and R2 are very close to unity for each case of l and this indicates that the correlation is very good. Then, the relationship between the optimum A value and the parameter l is established. As illustrated in Fig. 10,

$$A= -0.3\ln(l)+2.33. \quad (25)$$

The coefficient of correlation of equation (25), R^2, is 0.96. The fact that R^2 is close to unity verifies the accuracy of equation (25) to predict the effect of l on A.

Based on the above, finally the following expressions are proposed for the factors A and B of equation (22)

$$A = -0.3\ln(l)+2.33 \quad (26)$$
$$B=0.56$$

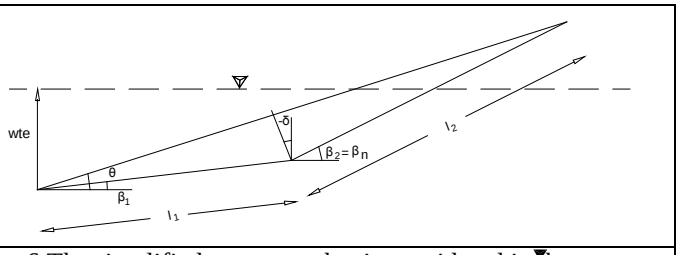

Fig. 6 The simplified geometry that is considered in the parametric analyses

VERIFICATION

Equation (22) with A and B given by equation (26) are first verified using all the analyses of figs. 7 and 8. Table 1 gives the validation in terms of the parameters β1, β2, θ, δ, l, wte, and c' (and φ'). The number of cases (N) and correlation (the factor C and the coefficient of correlation R^2 of equation (24)) for each case is given. It can be observed that in all cases the factor C and the coefficient of correlation R^2 are very close to unity, something the verifies the correctness of equation (22) with A and B given by equation (26)

DISCUSSION

Equation (22) with A and B given by equation (26) was obtained from only one applied excitation (the El-Centro earthquake) and one geometry type (Fig. 6). It is needed to study the ability of equation (22) with model parameters given by equation (26) to predict the effect of geometry changes on the seismic displacement under (1) different earthquakes and (2) complex geometries simulating actual slopes that have slid.

Table 1. Cases that were considered in the parametric analysis of the geometry of fig. 6 and the number of cases (N) and correlation (the factor C and the coefficient of correlation R^2) of the analytical solution for each case

Parameter	Values	N	Eqs. (22), (23)		Eqs. (22), (26)		
			C	R^2	N	C	R^2
β_1 (°)	-30	10	0.99	1.00	81	1.00	1.00
	-20	10	0.99	1.00			
	-10	10	1.00	1.00			
	0	10	1.00	1.00			
	5	11	0.99	1.00			
	10	10	1.00	1.00			
	20	10	1.00	0.99			
	29	10	1.00	0.99			
β_2(°)	31	9	1.00	0.99	50	1.00	1.00
	40	11	0.99	1.00			
	50	10	1.00	1.00			
	60	10	1.00	1.00			
	70	10	1.00	1.00			
δ(°)	-40	11	0.99	0.99	88	1.00	1.00
	-30	11	0.99	1.00			
	-20	11	0.99	1.00			
	-10	11	0.99	1.00			
	0	11	0.99	1.00			
	10	11	1.00	1.00			
	20	11	1.01	0.99			
	30	11	1.01	0.98			
θ(°)	10	20	0.99	1.00	72	1.00	1.00
	15	17	0.99	1.00			
	20	14	0.99	1.00			
	25	12	1.00	1.00			
	35	9	1.00	1.00			
l (m)	10	10	0.99	1.00	61	1.00	1.00
	20	11	0.99	1.00			
	60	10	0.99	1.00			
	100	10	0.99	0.97			
	300	10	0.99	0.97			
	1000	10	0.98	0.93			
C' (kPa) (and φ')	0	8	1.00	1.00	72	1.00	1.00
	2	11	1.00	1.00			
	4	14	1.00	1.00			
	6	19	1.00	1.00			
	8	20	1.00	1.00			
water table elev. (m)	0	9	1.00	1.00	90	1.00	1.00
	1	9	0.99	1.00			
	2	12	0.98	0.99			
	3	20	0.96	1.00			
	4	20	0.94	1.00			
	5	20	0.92	0.97			

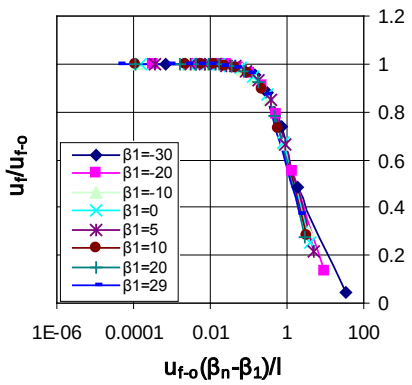

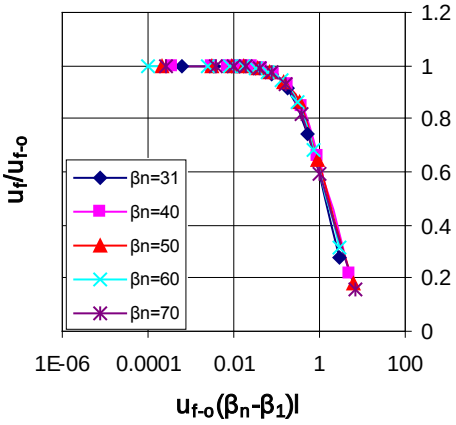

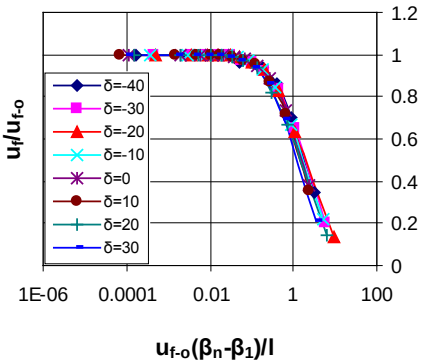

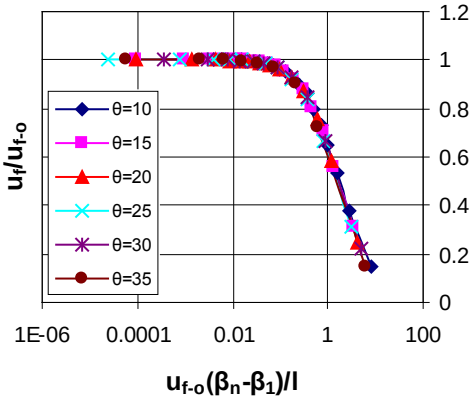

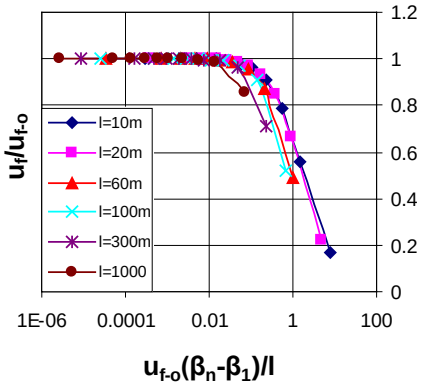

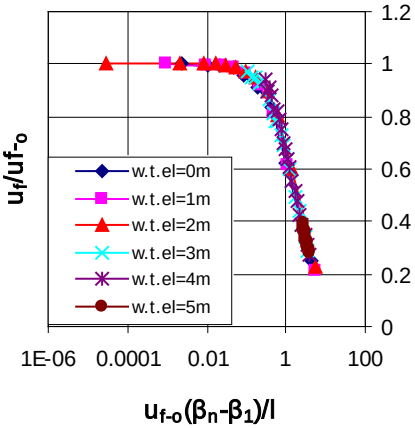

Fig. 7 The results of the parametric analyses. The effect of β1,βn=β2, δ, θ, l, water table elevation of the geometry of Fig. 6 in the relationship between the ratio (u_f/u_{f-o}) and the factor F.

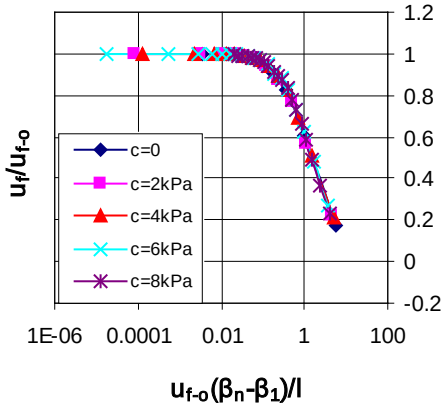

Fig. 8. The results of the parametric analyses. The effect of cohesion and friction of the geometry of Fig. 6 in the relationship between the ratio (u_f/u_{f-o}) and the factor F.

(a)

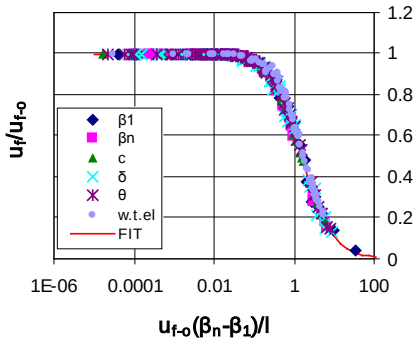

(b)

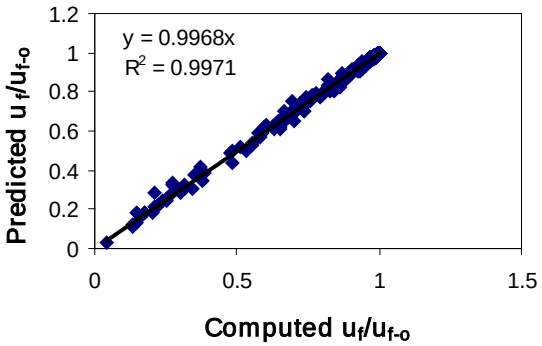

Fig. 9 The values of the coefficients A and B for the case of the geometry of Fig. 6 with l=20m and the El-Centro earthquake. All cases of Figs 7 and 8 are given, except for the case of varying δ.

Table 2. The parameter A best fitted the numerical results in terms of the slip length l of the geometry of Fig. 6 and the number of cases (N) and correlation (the factor C and the coefficient of correlation R^2) of the analytical solution for each case.

l (m)	A	C	R^2	N
10	1.7	0.99	1.00	10
20	1.5	0.99	1.00	11
60	1	1.00	0.99	10
100	0.8	0.99	0.99	10
300	0.55	1.00	0.99	10
1000	0.35	1.00	0.99	10

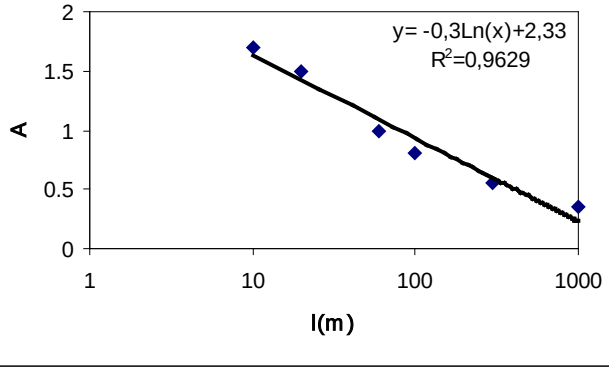

Fig. 10. The effect of the slip length on the factor A.

CONCLUSIONS

Newmark's sliding-block model is usually used for the prediction of permanent co-seismic displacements of slopes and earth structures. This model considers the motion of a block on an inclined plane with Mohr-Coulomb resistance. Recently, a multi-block method has been developed that considers a body sliding in n different inclinations. The method, unlike Newmark's sliding-block model, simulates the change in geometry of the slope towards a more stable configuration, which is the usual state in the field and affects the predictions when the seismic displacement is large. The paper studies the effect of the change in geometry of the slope towards a more stable configuration in the seismic displacement and using the multi-block model obtains equation (22) with parameters A and B given by equation (26) that correct Newmark's sliding-block predictions.

In particular, the methodology used to derive equations (22) and (26) is the following: (a) obtain a factor describing the effect of the change in geometry of the slope with displacement by formulating the equation of motion of the multi-block model for a simplified geometry, (b) by applying the multi-block model in the geometry of Fig. 6 in a parametric manner, investigate quantitavely the effect that the above factor has in the ratio (u_f/u_{f-o}), where u_f and u_{f-o} is the

final displacement predicted when geometry changes are and are not considered respectively and (c) formulate an empirical equation describing the effect computed in (b).

More specifically, in (a) the factor F (equation 20)) was obtained. The factor F tends to zero when (1) the seismic displacement is very small, (2) the length of the slip surface is very large and (3) the difference in inclination of the last (upper) and first (lower) blocks of the slip sub-planes of the slope is very small. In (b) the graphs of Figs 7 and 8 were obtained giving the effect of the parameters $\beta 1$, $\beta 2=\beta n$, δ, θ, l, wte (water table elevation), c' (and φ') of Fig. 6 on the relationship between the factor F and the ratio (u_f/u_{f-o}). In (c) equation (22) is proposed. From the results of (b) it is detected that the fitting parameters A and B of equation (22) are affected by the slip length l, but do not depend significantly on the remaining parameters of Fig. 6. Thus, the fitting parameters A and B were taken to vary only with l.

REFERENCES

Ambraseys N., Srbulov M. (1995). Earthquake induced displacements of slopes, Soil Dynamics and Earthquake Engineering; 14, pp. 59-71.

Gazetas G., P. Dakoulas (1992), “Seismic analysis and design of rockfill dams: State-of-the-Art”, Soil Dynamics and Eathquake Enginering Journal, 11, pp. 27-61.

Richards R. Jr., D. Elms (1979), “Seismic behavior of gravity retaining walls”, ASCE Proceedings,Journal Geotechnical Engineering Division, Vol. 105, GT4, pp. 449-464.

Dahliquist, G. and Bjorck, A., translated by Andeson, N. (1974). Numerical methods, Prentice-Hall Inc., New Jersey.

Ishibashi, Zhang, X. (1993), “Unified shear moduli and damping ratios of sand and clay”. Soils and foundations, Vol. 33, No 1, pp 182-191

Kramer S. (1996). Geotechnical Earthquake Engineering. Prentice-Hall, pp 438-447

Newmark, N. M. (1965). “Effects of earthquakes on dams and embankments.” Geotechnique, 15(2), 139-159.

Makdisi F. I. and H. B. Seed, (1978) “Simplified procedure for estimating dam and embankment earthquake-induced deformations”, ASCE Proceedings, Journal Geotechnical Engineering Division, Vol. 104, GT 7, pp. 849-867.

Modaressi, H., Aubry, D, Faccioli, E., Noret, C. (1995). Numerical modelling approaches for the analysis of earthquake triggered landslides. Proceedings: Third International Conference on Recent Advances in Geotechnical Earthquake Engineering and Soil Dynamics, April 2-7, Volume II, St. Louis, Missouri.

Sarma S.K. (1979). Stability analysis of embankments and slopes. Journal of Geotechnical Engineering ASCE; Vol.105, No. 12, pp. 1511-1524.

Sarma S.K. and Chlimitzas G. (2001). Analysis of seismic displacement of slopes using multi-block model. Final report performed under the grant of the European Commission Project ENV4-CT97-0392, January.

Sarma, S. K. (1999). "Seismic slope stability - The critical acceleration", Proceedings of the Second International Conference on Earthquake Geotechnical Engineering, Balkema, Lisbon, 1999, pp. 1077-1082.

Sarma, S.K. (1975). Seismic Stability of Earth Dams and Embankments”, Geotechnique, 1975, Vol. 25, No. 4, pp.743-761

Stamatopoulos, C. A. (1996) Sliding System Predicting Large Permanent Co-Seismic Movements of Slopes. Earthquake Engineering and Structural Dynamics, Vol. 25, No, 10, pp 1075-1093.

Stamatopoulos C. (1992). Analysis of a slide parallel to the slope. Proc. 2nd Greek National Conference of Geotechnical Engineering., Vol. 1, pp. 481-488. (in Greek)

Stamatopoulos C., Velgaki E., and Sarma S. (2000). "Sliding-block back analysis of earthquake induced slides". Soils and foundations, The Japanese Geotechnical Society, Vol. 40, No. 6, pp 61-75.

Stamatopoulos C. (2003). Dynamics of soils and foundations. Program: earthquake engineering and earthquake resistant structures. Hellenic Open University , Patras, Greece (in Greek).

Tika-Vassilikos Th, S. Sarma and N. N. Ambraseys (1993). “Seismic displacements on shear surfaces on cohesive soils”, Earthquake Eng. and Structural Dynamics, Vol. 22, pp. 709-721

Whitman R. V., (1993). Predicting earthquake-caused permanent deformations of earth structures, article on “Predictive Soil Mechanics”, Thomas Telford, London, pp. 729-741.